Past seismic slip-to-the-trench recorded in Central America megathrust

Paola Vannucchi[1,2], Elena Spagnuolo[3], Stefano Aretusini[4], Giulio Di Toro[4,5], Kohtaro Ujiie[6], Akito Tsutsumi[7], Stefan Nielsen[8]

[1] Department of Earth Sciences, Royal Holloway, University of London, Egham, UK
[2] Dipartimento di Scienze della Terra Università di Firenze, Firenze, Italy
[3] Sezione di Sismologia e Tettonofisica, Istituto Nazionale di Geofisica e Vulcanologia, Roma, Italy
[4] School of Earth, Atmospheric and Environmental Sciences, Manchester University, Manchester, UK
[5] Dipartimento di Geoscienze, Università di Padova, Padova, Italy
[6] Department of Geosciences, University of Tsukuba, Tsukuba, Japan
[7] Graduate School of Science, Kyoto University, Kyoto, Japan
[8] Department of Earth Sciences, University of Durham, Durham, UK

The 2011 Tohoku-Oki earthquake revealed that co-seismic displacement along the plate boundary megathrust can propagate to the trench. Co-seismic slip to the trench amplifies hazards at subduction zones, so its historical occurrence should also be investigated globally. Here we combine results from IODP Exp. 344 offshore SE Costa Rica with 3D reflection seismic interpretation and experimental data to identify and document a geologic record of past co-seismic slip-to-the-trench. IODP Exp. 344 drilled an old, < 1.9 Ma, megathrust frontal ramp – at ca. 325 mbsf – that superimposes older Miocene biogenic oozes onto late Miocene-Pleistocene silty clays. Stratigraphy and geophysical imaging constrain the position of the basal decollement to lie within the biogenic oozes.

Friction experiments show that when wet, silty clays and biogenic oozes are both slip-weakening at subseismic and seismic slip velocities. Oozes are stronger than silty clays at slip velocity ≤0.01 m/s, and wet oozes only become as weak as silty clays at slip velocity of 1 m/s. The implication is that the geological structures found in the forearc offshore SE Costa Rica were deformed during seismic slip-to-the-trench events. During slower aseismic creep, deformation would have preferentially localized within the silty-clays.

Geodetic data, seafloor bathymetry, and tsunami inversion modeling all indicate that the 2011 M_w 9 Tohoku-Oki earthquake ruptured to the trench, with 50-80 m co-seismic slip occurring across the shallow portion of the megathrust [1-3]. These exceptional datasets showed, for the first time, that ruptures can propagate to the trench during subduction megathrust earthquakes. Previously, this domain had been considered to only slip aseismically [4]. This observation immediately raises follow-on questions: Is there evidence that co-seismic slip to the trench has occurred in other subduction zones? What is the potential for other megathrusts to co-seismically rupture to the trench?

Following ocean drilling results in the Japan Trench [5], investigation has focused on the smectite-rich, pelagic clays recovered from the shallow portions of the Tohoku megathrust. Friction experiments showed that when the fault's original fabric is preserved, the Tohoku pelagic clays are cohesionless reducing fracture energy and favoring earthquake rupture propagation[6]. The very small fracture energy and shear stress of pelagic clays when sheared at seismic slip velocities (~1 m/s) can allow propagation of earthquake rupture from depth[7,8], explaining slip to the trench during the 2011 Tohoku-Oki earthquake[8]. On the ocean floor, deposition of pelagic sediments typically alternates between clays and biogenic oozes[9,10], with the latter mostly subducting in the eastern central and south Pacific (Fig. 1). In contrast to pelagic clays, biogenic oozes have been proposed to inhibit both fault rupture propagation and displacement during earthquakes, and so prevent the occurrence of tsunamis [9]. Laboratory friction experiments have suggested, however, that biogenic oozes may play a key role in earthquake nucleation at depth [11-13].

In this study we report evidence from ocean drilling in southern Costa Rica that biogenic oozes are the host sediment for the decollement at the trench. This observation, combined with the result from high-velocity friction experiments suggests that near-trench slip here was rapid, and likely tsunamigenic.

Studies of the shallower extents of subduction megathrusts have relied heavily on ocean drilling; only modern subduction systems offer a clear view of frontal prism geometry and the *in-situ* properties of the material involved in the fault zone. Integrated Ocean Drilling Program Expeditions 334 and 344, the Costa Rica Seismogenesis Project (CRISP), targeted both the incoming Cocos Plate sedimentary section at IODP Sites U1381 and U1414, and the frontal prism at Site U1412, the latter located ~3 km landward of the Middle America Trench (MAT) axis (Fig. 2A, B). The incoming plate sedimentary succession consists of Miocene pelagic biogenic oozes overlain by late Miocene to Pleistocene hemipelagic silty clays (Fig. 2C). At Site U1381 the oozes directly lie on Cocos Ridge basalt, while at Site U1414 a well-lithified layer of sandstone is interposed between the oozes and this basalt (Fig. 2C). Here, the thickness of the incoming plate sediment section varies considerably both along strike and down dip because of the rugged topography of the Cocos Ridge. Moving toward the frontal prism, reflection seismic profiles show a 5-10 km wide frontal accretionary prism [14] (Fig. 2A). The portion of the frontal prism drilled during IODP Exp. 344 at Site U1412 consists of Miocene pelagic biogenic oozes overlain by late Miocene to Pleistocene hemipelagic silty clays, both resting on top of younger Pleistocene silty clays (Fig. 2B). This stratigraphy implies that the frontal prism is indeed formed by oceanic sediments offscraped from the incoming plate and accreted through a series of thrusts at the front of the subduction margin (Fig. 2C). Most importantly, although Site U1412 did not reach the modern basal decollement, it drilled through a former frontal thrust. The thrust occurs between ≈321 and ≈329 mbsf, at the base of ≈120 m biogenic oozes. Although the actual thrust surface was not recovered, the core catcher of Core 344-U1412C-4R contained mixed Miocene and Pleistocene sediments, with no traces of the lithological units below the biogenic oozes.

This thrust is the ramp of a thrust system in which the biogenic oozes form the hangingwall. These are the youngest possible sediments that could be cut by the basal decollement, which means that the decollement propagated neither in the silty clays nor along the silty clay/biogenic ooze boundary. High-resolution 3D seismic reflection data[15] show ≈125 m thick underthrust sediments landward of Site U1414, where drilling shows the total thickness of the biogenic oozes is ≈180 m. This argues against the possibility that the basal decollement follows the basalt-oozes boundary.

The lack of seafloor crests and clear offsets to the lower slope deposits landward of the frontal thrust (Fig. 2A) supports the hypothesis of an imbricate stack of thrust sheets in which the frontal thrust remains active until a new frontal thrust forms seaward of it. The basal decollement propagates in the direction of slip along a weak surface, near the toe it can ramp up-section. Although Site U1412 did not reach the modern decollement, both the presence of this old frontal thrust and 3D seismic reflection imaging imply that biogenic oozes were the layer in which the megathrust propagated – i.e. the basal dècollement - beneath this accretionary prism (Fig. 2B).

The biogenic oozes are formed by various proportions of calcareous nannofossils, planktonic and benthonic foraminifera, radiolarians, diatoms and sponge spicules. The average mineralogical composition of our samples is 80% calcite and 20% amorphous silica (microfossils and tephra) for the biogenic ooze, and 30% calcite, 50% clay minerals, 20%

lithics (quartz and plagioclase) for the silty clays (Supplementary Figure 1). On average, the 50% clay mineral fraction contains 92% smectite (montmorillonite), 8% kaolinite, and <1% illite [16]. It might be anticipated from previous work on smectite-rich sediments that the abundance of smectite would imply that the silty clays should be the weaker layer in this oceanic sedimentary succession [8,17]. This stands in contrast with the geometric and drill evidence described above.

The presence of a frontal accretionary prism allows us to analyze the velocity-dependent frictional behavior of incoming sediment, and apply this knowledge to infer the mechanical behavior near the toe of the frontal prism built from these sediments (Fig. 2B). The CRISP setting is ideal to study the effect of slip velocity on sediments, because other factors that could cause their weakening, such as temperature and fluid-rock interactions, are negligible, in particular in biogenic oozes. At Site U1412, *in-situ* temperature measurements linearly extrapolated to the depth of the old frontal megathrust estimate T=40°C [18], while thermal models imply T<30°C [17]. Fluid overpressure can also weaken sediments as recently reported by experiments on material from the same Site U1414[12]. Both Site U1381 and U1414 show that biogenic oozes compact more slowly than silty clays. In particular at Site 1414 the porosity of the oozes - ≈50% on average - locally increases to ≈80% at ≈225 mbsf, before decreasing to the base of the sediments. Fluid-rich sediment layers have also been identified by reflection seismics to be located between the basement and the basal decollement[15]. However CRISP drilling recorded no signs of fluid overpressure across the old frontal thrust as well as in the incoming plate sections. Pore fluids extracted from sediments adjacent to the old frontal megathrust have lower than seawater salinity [18]. At Site U1412, the increasing Ca^{+2} content in the pore fluids with depth indicates that no diagenesis other than compaction has begun within drilled sediments [18]. Dissolved CO_2 and hydrocarbons were only measured in the upper silty clay unit of Site U1412: the most abundant species is methane – 0.65 vol% - while CO_2 is ~0.01vol% [18]. In the biogenic oozes this value is likely to be higher, however breakdown of organic matter and decarbonation of limestone are only expected to occur deeper than 60 km [19,20].

To determine the mechanical behaviour of sediments under appropriate P-T conditions for the frontal prism we conducted 23 experiments (Supplementary Notes) using the rotary shear machine 'SHIVA' [21]. Incoming plate sediments from Sites U1381 and U1414 were carefully powdered to a grain size < 250 μm to preserve intact most of the microfossil tests. Samples were dried to a maximum T of 50°C for 12 hours and rehydrated with distilled water to reproduce the relative moisture content of the original drill cores here expressed in percentage on weight of water/weight of bulk sample (i.e., 25 and 80 wt.% water content for silty clays and 50 wt.% water content for oozes)[18,22]. Powders were also sheared under room humidity conditions to provide a reference end-member. Experiments were all conducted at room temperature. Two millimeter thick layers of powders were confined within a ring-shaped (35-55mm int./ext. diameter) steel holder [23] and sheared under a constant normal stress σ_n = 5 MPa (equivalent to ~200 m depth) to reproduce shallow depth conditions. Fluid pressure can vary locally, due to the instantaneous frictional heating at seismic slip rates, although these pressure variations were not monitored. All mechanical results are therefore provided in terms of the recorded shear stress τ, which results in an effective friction coefficient $\mu^* = \tau / \sigma_n$ versus slip (D) and slip rate (V). All samples were initially sheared at 1×10^{-5} m/s for 10 mm to attain both compaction and the residual shear stress level (τ_0) to be used as initial condition for the experiments (pre-shear phase) and arguably as a proxy for the state of shear stress preceding earthquake rupture at the trench.

After this phase, a 300s hold was set before applying a constant velocity for 1 m and 3 m of total displacement at 0.01 and 1 m/s, the latter being close to the slip velocity calculated for the 2011 M_w 9 Tohoku-Oki earthquake [24], to the high-slip patches of tsunami earthquakes in Nicaragua and Peru [25,26], and to values from dynamic rupture simulations of near-trench seismic slip [27].

The residual shear stress (τ_0) recorded at the end of the pre-shear phase is well reproduced for the silty clays for all experiments, with standard deviations *std* < 0.15 MPa. Biogenic oozes have the largest variations (Fig. 3A, B and Supplementary Notes) with *std* as large as 0.28 MPa (Fig. 3B 3A, B). In general, reproducibility is worse in biogenic oozes than in silty clays. This may be caused by the heterogeneity of the biogenic material forming the oozes. In the pre-shear phase both silty clays and oozes show slip-weakening and slip-strengthening behavior (Fig. 3A, B). Wet oozes are overall stronger than wet silty clays, in agreement with previous observations for slip velocities $<3x10^{-4}$ m/s [13].

At 0.01 m/s water content plays a major role. Under room-humidity conditions and during the initial acceleration stage, silty clays and biogenic oozes have a similar peak in shear stress (τ_p=3.31 ± 0.04 MPa and τ_p=3.27 ± 0.33 MPa respectively) (Fig. 3A). With increasing slip, both materials have a slip-weakening behavior within the first 0.05 m of slip, followed by slip-strengthening (Fig. 3A). In the presence of water, silty clays become clearly weaker than biogenic oozes. The frictional sliding behavior of wet silty clays is quite reproducible, with an initial decay that becomes nearly slip-neutral to slightly slip-strengthening reaching a steady-state shear stress τ_{ss} = 0.83 $\pm$ 0.02 MPa at 25% wt. H_2O. Biogenic oozes are slip weakening over the entire duration of the experiment but have an initial stage of abrupt weakening followed by a recovery stage during the first 0.02 m of slip before reaching τ_{ss} = 1.34 ± 0.19 MPa at 50% wt. H_2O.

At 1 m/s and room humidity conditions all samples have initial slip-weakening behavior (Fig. 3B) with a similar peak in shear stress (τ_p~ 3.45 MPa) after the initial acceleration stage. However, the shear stress decays faster in biogenic oozes than in silty clays and persists to a slightly higher steady-state value calculated at the end of each test (τ_{ss}=2.22± 0.26 MPa for oozes vs. τ_{ss}=1.76 ± 0.22 MPa for silty clays). In the presence of water, the experiments on oozes show peaks of shear stress similar to those at room humidity conditions with an average of τ_p=3.41 ± 0.33 MPa, but present an abrupt weakening stage before reaching a steady state value of τ_{ss}=0.57± 0.05 MPa (Fig. 3B). The peak shear stress for silty clays is weaker (τ_p=1.67 ± 0.14 MPa, 25% wt.H_2O and τ_p=1.45 ± 0.04 MPa, 80% wt.H_2O), decay is characterized by a short (flash) initial weakening followed by a slow stage of strengthening before further reduction to the steady state value (τ_{ss}=0.68 ± 0.06 MPa, 25% wt.H_2O and τ_{ss} =0.56 ± 0.01 MPa, 80% wt.H_2O).

The above experiments have shown that, during the onset of seismic slip-rates (1 m/s), biogenic oozes are always slip-weakening. Importantly, at lower slip rates (≤0.01 m/s) wet silty clays are weaker than oozes (Fig.3A), and deformation would localize more easily by creeping within silty clays than within biogenic oozes while the two fault materials become similarly weak at seismic slip-rates (Fig. 3B).

However, sliding friction alone does not control the onset of slip during an earthquake. Indeed an energy balance[28,29] (Supplementary notes Eq. S1) indicates that seismic rupture can occur when the elastic strain energy release *E* (which does increase with τ_0) equals or exceeds the summed dissipation of both fracture energy G_f (depending on τ_p and τ_{ss}) and sliding friction work W_f (depending on τ_{ss}). Any excess energy $E_r=E-(G_f+W_f)$ is then available for wave radiation, and under similar circumstances, faults with larger E_r are more likely to slip seismically. As noted above, biogenic oozes have a sharp slip weakening behaviour while silty clays are slip strengthening before decaying to steady state. Therefore, both the occurrence of strengthening in the silty clays and the stronger value of the residual shear stress (τ_0) in oozes are relevant factors to the propagation of slip.

Using τ_0 measured in the slow (10 µm/s) slip experiments (Fig. S2 of the Supplementary Notes) as a proxy of pre-seismic stress on the fault, we estimate values of the excess energy E_r from 23 experiments (Table S1 in Supplementary notes). At 0.01 m/s, E_r is similar for both silty clays and oozes (with the exception of one wet experiment in oozes, Fig. 3C), suggesting that slip can propagate easily in both types of sediments. However, at 1 m/s, wet oozes have a much higher residual stresses τ_0 than wet silty clays. Therefore oozes are prone to larger strain energies E and capable of accumulating the elastic strain required to produce a "locked" patch on a plate interface at shallow depths [30] (provided that the elastic strain is not released by adjacent weaker lithological units).

Recent experiments on material from the same Site U1414 suggest that at T between 70° and 140°C and P_f=120 MPa subduction thrust earthquakes would preferentially nucleate in biogenic oozes instead of silty clays [12]. If this is true, once rupture is initiated it could then propagate updip along the oozes, as documented from the drilling results. However, in southern Costa Rica, thermal modelling predicts that T>70°C are only to be expected at distances > 25 km from the trench [17], in a region where subduction erosion predominates [31]. Therefore, while the velocity-related friction behavior of the oozes vs. silty clays is relevant for the 5-10 km wide frontal accretionary prism, at the depths of earthquake nucleation, the host material would be expected to be upper plate rocks instead of these sediments.

Finally, lab measured yield stresses for the oozes and silty clays are easily both exceeded in nature by the stress transient associated with fault propagation near the trench during a megathrust earthquake as inferred by the stress drop values of the 2011 M_w 9 Tohoku-Oki earthquake [32] or the Peru and Nicaragua tsunami earthquakes (Fig. 1) [26,33].

These combined geological, geophysical and mechanical observations imply that the thrusts found in the forearc toe offshore SE Costa Rica were active during transient high slip-rates (i.e., rates only possible during earthquake slip to the trench).

The geological and mechanical observations discussed in this paper imply that the subduction of biogenic oozes has the potential to create the conditions for earthquake slip to the trench that will greatly amplify the tsunami hazard in this and many other subduction systems, in particular along the Cocos and Nazca subduction zones (Fig. 1). Our observations indicate that biogenic oozes can provide a valuable record of past slip-to-the-trench, and that past slip events can be effectively assessed locally by drilling into frontal prisms in high seismic and tsunami hazard areas.

References

1 Ito, Y. *et al.* Frontal wedge deformation near the source region of the 2011 Tohoku-Oki earthquake. *Geophysical Research Letters* **38**, doi:10.1029/2011gl048355 (2011).

2 Fujiwara, T. *et al.* The 2011 Tohoku-Oki Earthquake: Displacement Reaching the Trench Axis. *Science* **334**, 1240-1240, doi:10.1126/science.1211554 (2011).

3 Satake, K., Fujii, Y., Harada, T. & Namegaya, Y. Time and Space Distribution of Coseismic Slip of the 2011 Tohoku Earthquake as Inferred from Tsunami Waveform Data. *Bulletin of the Seismological Society of America* **103**, 1473-1492, doi:10.1785/0120120122 (2013).

4 Wang, K. L. & Hu, Y. Accretionary prisms in subduction earthquake cycles: The theory of dynamic Coulomb wedge. *Journal of Geophysical Research* **111**, B06410, doi:06410.01029/02005JB004094 (2006).

5 Chester, F. M. *et al.* Structure and Composition of the Plate-Boundary Slip Zone for the 2011 Tohoku-Oki Earthquake. *Science* **342**, 1208-1211, doi:10.1126/science.1243719 (2013).

6 Ikari, M. J., Kameda, J., Saffer, D. M. & Kopf, A. J. Strength characteristics of Japan Trench borehole samples in the high-slip region of the 2011 Tohoku-Oki earthquake. *Earth and Planetary Science Letters* **412**, 35-41, doi:dx.doi.org/10.1016/j.epsl.2014.12.014 (2015).

7 Faulkner, D. R., Mitchell, T. M., Behnsen, J., Hirose, T. & Shimamoto, T. Stuck in the mud? Earthquake nucleation and propagation through accretionary forearcs. *Geophys. Res. Lett.* **38**, L18303, doi:10.1029/2011GL048552 (2011).
8 Ujiie, K. *et al.* Low Coseismic Shear Stress on the Tohoku-Oki Megathrust Determined from Laboratory Experiments. *Science* **342**, 1211-1214, doi:10.1126/science.1243485 (2013).
9 Moore, J. C., Plank, T. A., Chester, F. M., Polissar, P. J. & Savage, H. M. Sediment provenance and controls on slip propagation: Lessons learned from the 2011 Tohoku and other great earthquakes of the subducting northwest Pacific plate. *Geosphere* **11**, 533-541, doi:10.1130/ges01099.1 (2015).
10 Horn, D. R., Horn, B. M. & Delach, M. N. Sedimentary Provinces of the North Pacific. *Geological Society of America Memoirs* **126**, 1-22, doi:10.1130/MEM126-p1 (1970).
11 Ikari, M. J., Niemeijer, A. R., Spiers, C. J., Kopf, A. J. & Saffer, D. M. Experimental evidence linking slip instability with seafloor lithology and topography at the Costa Rica convergent margin. *Geology* **41**, 891-894, doi:10.1130/g33956.1 (2013).
12 Kurzawski, R. M., Stipp, M., Niemeijer, A. R., Spiers, C. J. & Behrmann, J. H. Earthquake nucleation in weak subducted carbonates. *Nature Geoscience*, doi:10.1038/NGEO2774 (2016).
13 Namiki, Y., Tsutsumi, A., Ujiie, K. & Kameda, J. Frictional properties of sediments entering the Costa Rica subduction zone offshore the Osa Peninsula: implication for fault slip in shallow subduction zones. *Earth, Planets and Space* **66**, doi:10.1186/1880-5981-66-72 (2014).
14 Arroyo, I. G., Grevemeyer, I., Ranero, C. R. & von Huene, R. Interplate seismicity at the CRISP drilling site: The 2002 Mw 6.4 Osa Earthquake at the southeastern end of the Middle America Trench. *Geochemistry Geophysics Geosystems* **15**, 3035-3050, doi:10.1002/2014gc005359 (2014).
15 Bangs, N. L., McIntosh, K. D., Silver, E. A., Kluesner, J. W. & Ranero, C. R. Fluid accumulation along the Costa Rica subduction thrust and development of the seismogenic zone. *Journal of Geophysical Research-Solid Earth* **120**, 67-86, doi:10.1002/2014jb011265 (2015).
16 Charpentier, D. *et al.* in *AGU Fall 2013 Meeting* Vol. Abstract T34C-04 (San Francisco, 2013).
17 Kameda, J. *et al.* Pelagic smectite as an important factor in tsunamigenic slip along the Japan Trench. *Geology* **43**, 155-158, doi:10.1130/g35948.1 (2015).
18 Harris, R. N., Sakaguchi, A., Petronotis, K. & the Expedition 344 Scientists. Vol. 344 (Integrated Ocean Drilling Program, College Station, TX, 2013).
19 Gorman, P. J., Kerrick, D. M. & Connolly, J. A. D. Modeling open system metamorphic decarbonation of subducting slabs. *Geochemistry Geophysics Geosystems* **7**, doi:10.1029/2005gc001125 (2006).
20 Kerrick, D. M. & Connolly, J. A. D. Metamorphic devolatilization of subducted marine sediments and the transport of volatiles into the Earth's mantle. *Nature* **411**, 293-296, doi:10.1038/35077056 (2001).
21 Di Toro, G. *et al.* From field geology to earthquake simulation: a new state-of-the-art tool to investigate rock friction during the seismic cycle (SHIVA). *Rendiconti Lincei* **21**, 95-114, doi:10.1007/s12210-010-0097 (2010).
22 Vannucchi, P., Ujiie, K., Stroncik, N. & the Expedition 334 Scientists. Vol. 334 (Integrated Ocean Drilling Program Management International, Inc., Tokyo, 2012).
23 Smith, S. A. F. *et al.* Coseismic recrystallization during shallow earthquake slip. *Geology* **41**, 63-66 (2013).
24 Uchide, T. High-speed rupture in the first 20 s of the 2011 Tohoku earthquake, Japan. *Geophys. Res. Lett.* **40**, 2993–2997, doi:10.1002/grl.50634 (2013).
25 Piatanesi, A., Tinti, S. & Gavagni, I. The slip distribution of the 1992 Nicaragua earthquake from tsunami run-up data. *Geophys. Res. Lett.* **23**, 37-40, doi:10.1029/95GL03606 (1996).
26 Ihmle, P. F., Gomez, J.-M., Heinrich, P. & Guibourg, S. The 1996 Peru tsunamigenic earthquake: broadband source process. *Geophys. Res. Lett.* **25**, 2691-2694 (1998).

27 Hirono, T. *et al.* Near-trench slip potential of megaquakes evaluated from fault properties and conditions. *Scientific Reports* **6**, doi:10.1038/srep28184 (2016).
28 Andrews, D. J. Rupture velocity of plane strain shear cracks. *Journal of Geophysical Research* **81**, 5679-5687, doi:10.1029/JB081i032p05679 (1976).
29 Kanamori, H. & Rivera, L. in *Earthquakes: Radiated Energy and the Physics of Faulting* Vol. 170 *Geophysical Monograph Series* (eds R. Abercrombie, A. McGarr, G. DiToro, & H. Kanamori) 3-13 (2006).
30 LaFemina, P. *et al.* Fore-arc motion and Cocos Ridge collision in Central America. *Geochemistry Geophysics Geosystems* **10**, Q05S14, doi:10.1029/2008GC002181 (2009).
31 Vannucchi, P. *et al.* Rapid pulses of uplift, subsidence, and subduction erosion offshore Central America: Implications for building the rock record of convergent margins. *Geology* **41**, 995-998, doi:10.1130/G34355. (2013).
32 Brown, L., Wang, K. & Sun, T. Static stress drop in the Mw 9 Tohoku-oki earthquake: Heterogeneous distribution and low average value. *Geophys. Res. Lett.* **42**, 10,595-510,600, doi:10.1002/2015GL066361 (2015).
33 Satake, K. Mechanism of the 1992 Nicaragua tsunami earthquake. *Geophys. Res. Lett.* **21**, 2519-2522 (1994).

Acknowledgements

This research used samples and data provided by the International Ocean Drilling Program (IODP) (www.iodp.org/access-data-and-samples). The JOIDES Resolution crew and IODP technical team are thanked for their contributions during EXP. 334 and 344. PV acknowledges support during and following the Expeditions from IODP-Italia, J-DESC, and UK-IODP (Rapid Response Grant). ES, SA, SN and GDT acknowledge the ERC CoG project 614705 "NOFEAR". PV greatly benefitted from discussions with Jason Phipps Morgan. Michael Stipp and an anonymous reviewer are thanked for their constructive comments that significantly improved the paper. The data that support the findings of this study are available at 10.5281/zenodo.1003548.

Author contributions

PV described the cores in ODP Leg 170 and Leg 205, IODP Exp. 334 and Exp. 344, sampled the sediments used for the experiments described in this paper, contributed to their interpretation, and wrote the text. ES conducted the experiments and with the first author contributed to their interpretation, wrote the supplementary notes and prepared the files for the data repository. SA conducted the experiments and contributed to their interpretation. KU and AT described the cored in IODP Exp. 334 and performed an early set of experiments. GDT and SN contributed to the interpretation of the experiments.

The authors of the present manuscript declare that they have no competing financial interests.

Corresponding author: paola.vannucchi@rhul.ac.uk

Figure Captions

Figure 1

Distribution and thickness of Biogenic Oozes (mostly carbonaceous) on the Cocos and Nazca plates as calculated by DSDP-ODP-IODP drilling results. The blue italic numbers next to the circles indicate the DSDP-ODP-IODP drilling site used for the isopach map. Note that our interpolation does not consider bathymetry variations.

Figure 2

Location of ODP Leg 170 and IODP Exp. 334 and 344 (CRISP) offshore Central America. A) Post-stack depth migrated seismic section centered at the trench along Site U1381/Site U1412 transect (detail of BGR99 Line 7) [14]. B) Detail of Site U1412 location and recovered material. C) Stratigraphy of the drilled sites and conceptual cartoon of the accretionary system at the front of the CRISP transect as implied by the offshore drilling showing the detachment layer localized within the biogenic oozes – Note the lateral and downdip variation of the sediment thickness: in particular the biogenic oozes are ca. 50 m at Site U1381, ca. 180 m at Site U1414 – this site is projected from the position indicated in the location map, therefore its thickness in the cross section is not the effective drilled thickness, which is reported in the log -, and ca. 120 m at Site U1412. The location of the samples used for the friction tests is also shown.

Figure 3

Summary of experimental results. Different colors refer to different water content (see legend). **A**. Example shear stress as a function of slip obtained for low-velocity – 0.01 m/s – experiments for silty clays and biogenic oozes for different water content. The first 10 mm of slip are tested at 10 µm/s. **B**. Example shear stress as a function of slip obtained for high slip-velocity – 1 m/s – experiments for silty clays and biogenic oozes. The first 10 mm of slip are tested at 10 µm/s. At room humidity (RH) conditions, both silty clays and oozes show a slip weakening behavior, with comparable values of both peak and steady-state shear stress. Weakening, though, is very abrupt and pronounced for the oozes. Under wet conditions the peak shear stress for the silty clays is lower than the oozes, but silty clays show an initial slip strengthening behavior. At steady state conditions the shear stress is very similar for both materials. **C**. Excess energy $E_r=E-(W_f+G_f)$ available for rupture propagation and wave radiation, calculated from the experimental data (see Supplementary Notes). Empty and full circles refer to 1 m and 3 m of slip respectively.

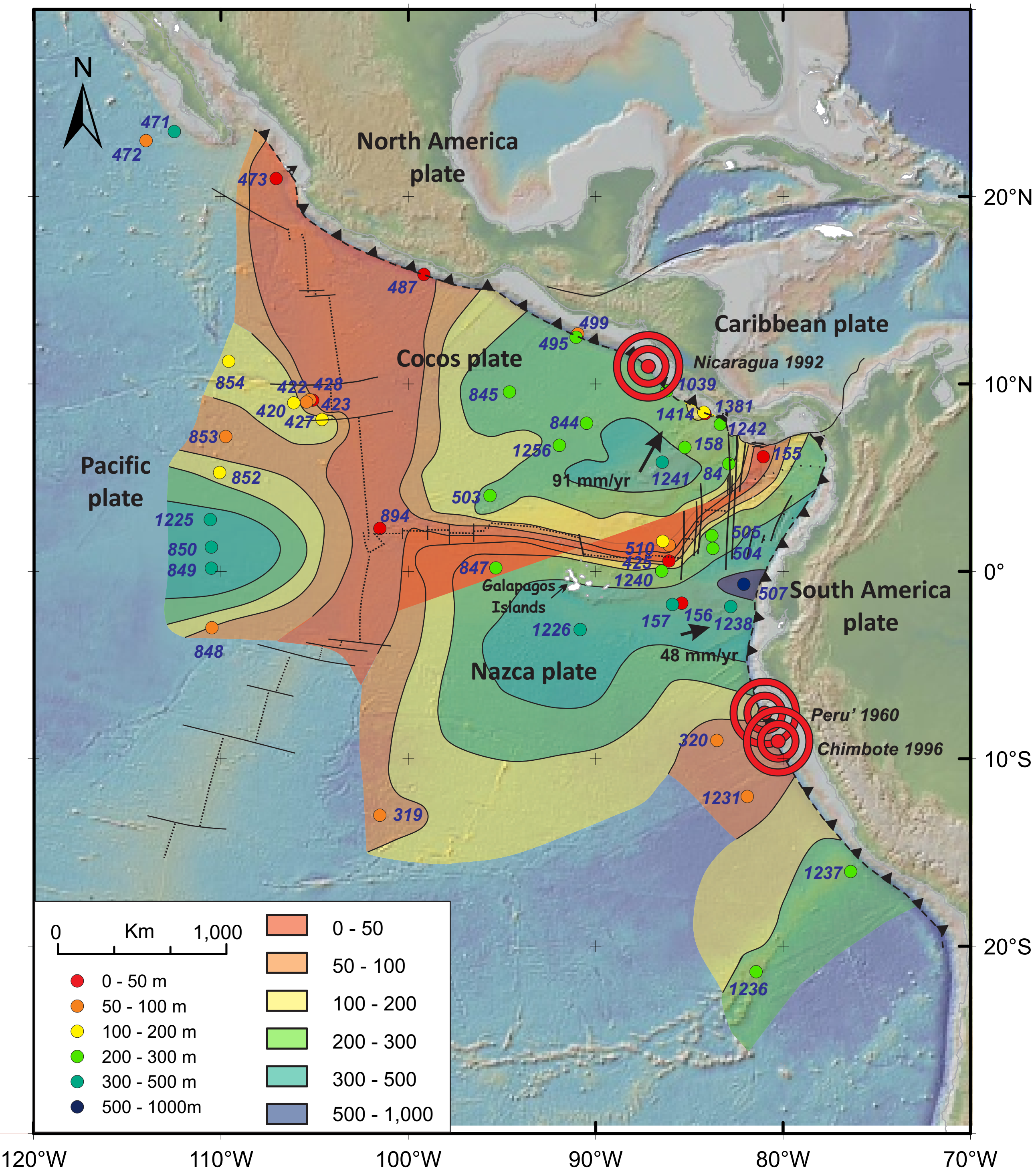

N
North America plate
Caribbean plate
Cocos plate
Pacific plate
Nazca plate
South America plate
Nicaragua 1992
Peru' 1960
Chimbote 1996
Galapagos Islands
91 mm/yr
48 mm/yr
471
472
473
487
499
495
854
422
428
423
420
427
853
852
1225
850
849
848
845
844
1256
503
894
847
1039
1414
1381
1242
158
155
1241
84
505
504
510
425
1240
507
157
156
1238
1226
320
1231
319
1237
1236
0 Km 1,000
0 - 50 m
50 - 100 m
100 - 200 m
200 - 300 m
300 - 500 m
500 - 1000m
0 - 50
50 - 100
100 - 200
200 - 300
300 - 500
500 - 1,000
20°N
10°N
0°
10°S
20°S
120°W
110°W
100°W
90°W
80°W
70°W

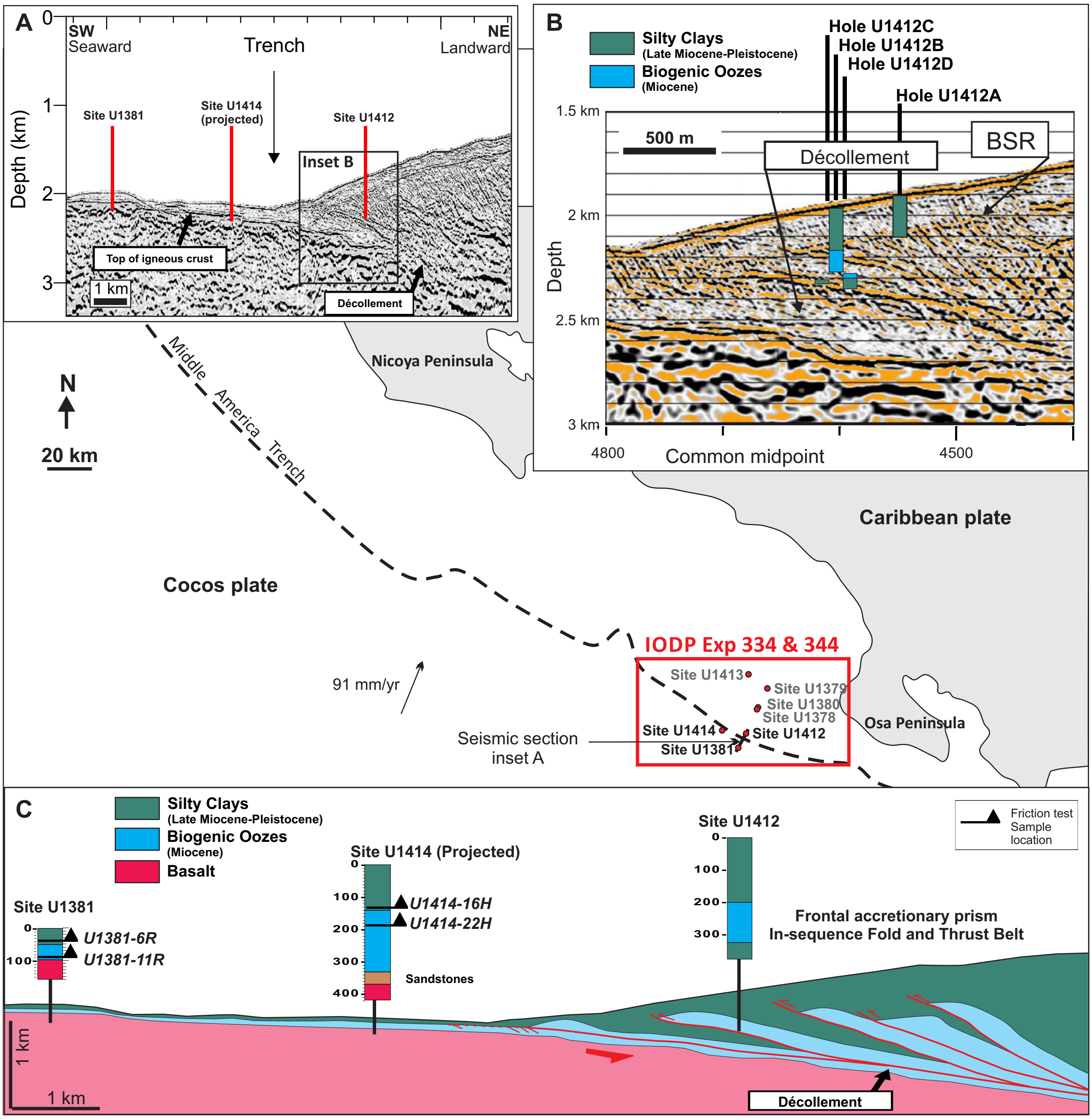
A
SW
Seaward
Trench
NE
Landward
Depth (km)
Site U1381
Site U1414 (projected)
Site U1412
Inset B
Top of igneous crust
1 km
Décollement
B
Silty Clays
(Late Miocene-Pleistocene)
Biogenic Oozes
(Miocene)
Hole U1412C
Hole U1412B
Hole U1412D
Hole U1412A
1.5 km
500 m
Décollement
BSR
2 km
Depth
2.5 km
3 km
4800
Common midpoint
4500
Nicoya Peninsula
N
20 km
Middle America Trench
Caribbean plate
Cocos plate
IODP Exp 334 & 344
Site U1413
Site U1379
Site U1380
Site U1378
91 mm/yr
Osa Peninsula
Seismic section
inset A
Site U1414
Site U1412
Site U1381
C
Silty Clays
(Late Miocene-Pleistocene)
Biogenic Oozes
(Miocene)
Basalt
Friction test
Sample
location
Site U1412
Site U1414 (Projected)
Site U1381
U1381-6R
U1381-11R
U1414-16H
U1414-22H
Sandstones
Frontal accretionary prism
In-sequence Fold and Thrust Belt
1 km
1 km
Décollement

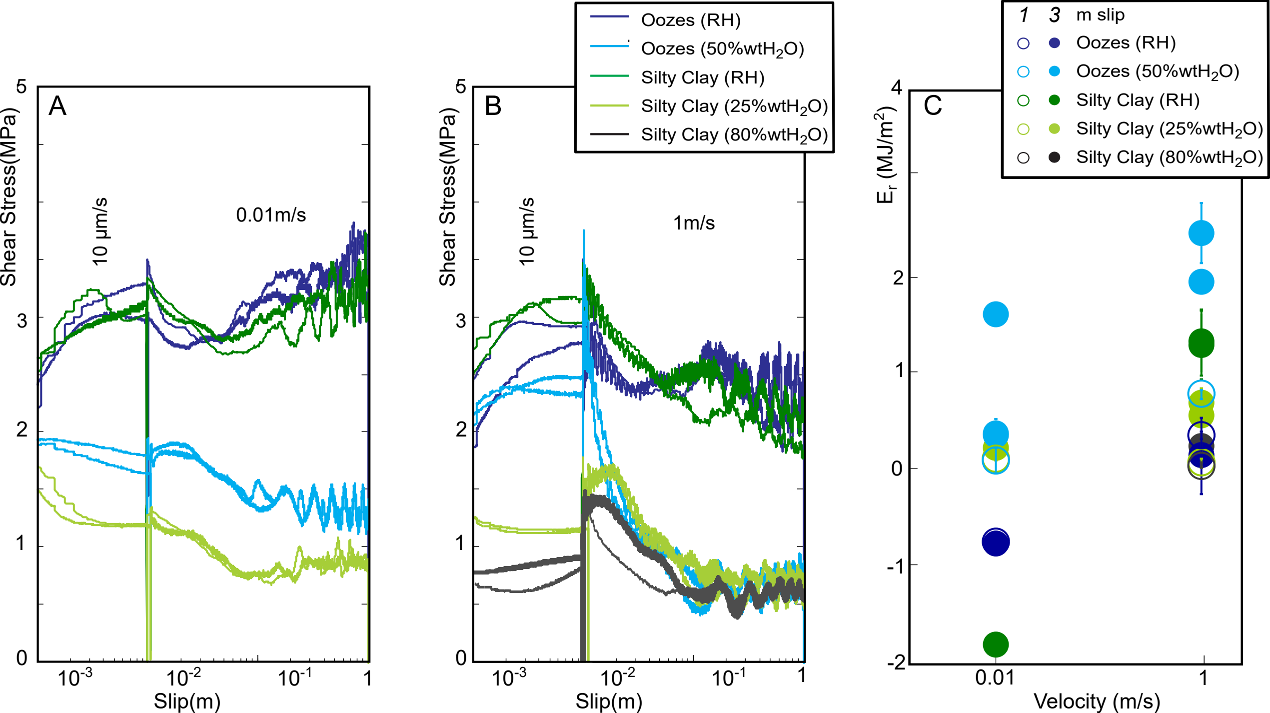

Oozes (RH)
Oozes (50%wtH2O)
Silty Clay (RH)
Silty Clay (25%wtH2O)
Silty Clay (80%wtH2O)
A
Shear Stress(MPa)
10 μm/s
0.01m/s
Slip(m)
B
1m/s
C
1 3 m slip
Er (MJ/m2)
Velocity (m/s)
0.01
1